LATITUDINAL TRENDS OF ANOMALOUS CRATERS OBSERVED WITH LRO MINI-RF RADAR DATA. B. J. Thomson[1], S. S. Bhiravarasu[2], C. Nypaver[1], C. D. Neish[3,4,] G. W. Patterson[5], P. Prem[5], and E. Heggy[6,6], [1]Dept. of Earth and Planetary Sciences, University of Tennessee, Knoxville, TN USA (bthom@utk.edu), [2]Lunar and Planetary Institute, Universities Space Research Association, Houston, TX USA, [3]The Planetary Science Institute, Tucson, AZ USA, [4]The University of Western Ontario, London, ON, Canada, [5]Planetary Exploration Group, Johns Hopkins University Applied Physics Laboratory, Laurel, MD, [6]Viterbi School of Engineering, University of Southern California, Los Angeles, CA, [7]Jet Propulsion Laboratory, California Institute of Technology, Pasadena, CA.

Introduction: The radar polarimetric signature for thick (multiple radar wavelength), relatively pure deposits of water ice has been detected on numerous planetary bodies such as the icy moons of Jupiter [e.g., 1]. Even inside the Solar System's frost line, ice can be stable and detectable with radar in the polar environments of atmosphereless bodies with low obliquity, such as Mercury [e.g., 2, 3]. However, radar signatures of silicate-ice mixtures are non-unique, leading to multiple conflicting interpretations for polarimetric measurements of environments like the lunar poles (e.g., whether the observed polarimetric properties are due ice [4-6] or roughness [7-9]).

Impact craters near the poles of the Moon have long been theorized to potentially harbor lunar volatiles [10, 11] and have been the subject of numerous investigations [e.g., 12, 13-17]. Using Mini-SAR S-band radar data from the Chandrayaan-1 mission [4], a number of small craters 5 to 15 km in diameter were initially identified as "anomalous" in that they exhibit elevated circular polarization ratio (CPR) values in their interior but not their exterior. This is in contrast to fresh impact craters, which exhibit high CPR values both in their interior and exterior due to rough, rocky ejecta. This observation was expanded upon with LRO (Lunar Reconaissance Orbiter) Mini-RF S-band data, and it was noted that although the interior crater CPR enhancements are not large enough to be a unique discriminator of ice, the number of anomalous craters is higher at the poles than elsewhere [6, 18]. However, a recent study of the radar properties of a global distribution of craters has questioned this finding [9]. Here we reexamine the radar data for lunar anomalous impact craters as a function of latitude.

Methods: This work utilizes the global lunar crater catalog assembled by [19] that contains 22,746 craters that range in diameter from 5–20 km. Craters in this catalog were identified manually by [19] using a combination of LROC WAC mosaics and the LOLA-LROC merged topographic product GLD100 [20]. Using ESRI's ArcMap software, we extracted median CPR values from crater interiors and exteriors from all craters in the catalog out to 1.414 crater radii; this outer limit was chosen so that an equal area would be considered inside and outside the craters. Data for craters between ±60° latitude were extracted using a simple cylindrical projection, while polar stereographic projections were used for the poles. We then took the difference between the interior and exterior CPR values for craters that that were more than 50% covered by Mini-RF data.

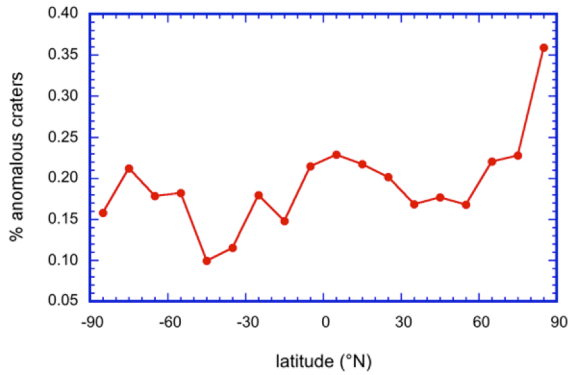

Figure 1. Percentage of lunar craters 5–20 km in diameter observed to be anomalous (ΔCPR interior – exterior ≥ 0.1) as a function of latitude.

Results: As a cutoff value for the definition of an anomalous crater, we used a threshold difference of 0.1 between the median interior and exterior CPR values following [9] (i.e., anomalous craters have ΔCPR interior – exterior ≥ 0.1). **Figure 1** gives the percentage of the crater population that meets this definition of anomalous as a function of latitude in 10° latitude bins.

The percentage of craters classified as anomalous in non-polar regions (between 70°S and N) has a mean value of about 18±4%, or about one-fifth of the total crater population is this size range. This finding is in consistent with a recent study that measured radial CPR profiles of 6,206 craters between 0.8–2 km in diameter [21]. Craters in that study became more anomalous-looking as they reach middle age (~1.5–2.5 Ga), meaning that all craters pass through an anomalous-looking phase as results of typical degradational processes and regolith gardening. The observed uptick in the percentage of anomalous craters in the north polar region (**Fig. 1**) supports the previous interpreta-

tions [4, 6, 18] that anomalous craters are overabundant relative to non-polar areas.

A somewhat unexpected finding is that the percentage of anomalous craters in the south polar region (80 to 90°S) was not enhanced similar to the north. The LRO rolled observations of Shackleton were not included in the south polar mosaic since they were acquired at reduced angles of incidence. Yet this south-north difference is in line with earlier findings: using Chandrayaan-1 Mini-SAR data [4], 35 anomalous craters were identified in the north polar area and 15 in the south polar region within 20° of the pole (i.e., ±70° to 90°), which is more than a factor of two difference between the two poles. The higher spatial resolution data from Mini-RF revealed additional anomalous craters in both polar regions, bringing the total number up to 43 anomalous craters in the north pole mosaic and 28 anomalous craters in the south pole mosaic [6] (a difference of about 1.5).

If one were to fold the data given in **Figure 1** about the equator and combine data from north and south latitudes bins, the north polar excess of anomalous craters would be reduced (as was done by [9] in their Fig. 5). However, the geologic environments of each pole, while similar, are distinct. While both polar regions exhibit average radar backscatter properties typical for the highland areas of the Moon [e.g., 22, 23], the south polar region is dominated by the rim of the SPA (South-Polar Aiken) basin and is topographically rougher (e.g., it has a higher median slope at ~17 m baselines [24]). The illumination [25], thermal conditions [26], and distribution of predicted ice stability depths [27] at the two poles also differ. Given these differences, it seems prudent to consider them independently. The source of the north-south asymmetry in the abundance of the anomalous craters remains to be explained, but the claim that both polar regions are not statistically different from non-polar regions does not appear to hold (i.e., 36% anomalous craters ≠ 18±4%). A role for ice in the abundance of CPR anomalous craters therefore cannot be excluded.

Acknowledgements: This work was funded in part by grant NNX17AI80G from the NASA Lunar Data Analysis program.

References: [1] Ostro S.J. and Shoemaker E.M. (1990) *Icarus*, *85*, 335-345. [2] Slade M.A. et al. (1992) *Science*, *258*, 635-640. [3] Harmon J.K. et al. (2011) *Icarus*, *211*, 37-50. [4] Spudis P.D. et al. (2010) *GRL*, *37*, L06204. [5] Thompson T.W. et al. (2011) *JGR*, *116*, E01006. [6] Spudis P.D. et al. (2013) *JGR*, *118*, 2016-2029. [7] Fa W. and Cai Y. (2013) *JGR*, *118*, 1582-1608. [8] Eke V.R. et al. (2014) *Icarus*, *241*, 66-78. [9] Fa W. and Eke V.R. (2018) *JGR*, *123*, 2119-2137. [10] Arnold J.R. (1979) *JGR*, *84*, 5659-5668. [11] Watson K. et al. (1961) *JGR*, *66*, 3033-3045. [12] Paige D.A. et al. (2010) *Science*, *330*, 479-482. [13] Gladstone G.R. et al. (2012) *JGR*, *117*, E00H04. [14] Mitrofanov I. et al. (2012) *JGR*, *117*, E00H27. [15] Feldman W.C. et al. (1998) *Science*, *281*, 1496. [16] Colaprete A. et al. (2010) *Science*, *330*, 463-468. [17] Li S. et al. (2018) *PNAS*, *115*, 8907-8912. [18] Thomson B.J. et al. (2012) *LPS XLIII*, Abstract #2104. [19] Povilaitis R. et al. (2018) *PSS*, *162*, 41-51. [20] Scholten F. et al. (2012) *JGR*, *117*. [21] Fassett C.I. et al. (2018) *JGR*. [22] Cahill J.T.S. et al. (2014) *Icarus*, *243*, 173-190. [23] Campbell D.B. et al. (2006) *Nature*, *443*, 835-837. [24] Rosenburg M.A. et al. (2011) *JGR*, *116*, E02001. [25] Mazarico E. et al. (2011) *Icarus*, *211*, 1066-1081. [26] Hayne P.O. et al. (2015) *Icarus*, *255*, 58-69. [27] Siegler M. et al. (2016) *Nature*, *531*, 480-484.